(11) Meier, D. J. In "Block and Graft Copolymers"; Burke, J. J., Weiss, V., Eds.; Syracuse University Press: Syracuse, N.Y., 1973.
(12) Meier, D. J. Proceedings, Polymer Colloquium, Kyoto, Japan, Sept 1977.
(13) Mayer, R. *Polymer* **1974**, *15*, 137.
(14) Eastmond, G. C.; Phillips, D. G. *Polymer* **1979**, *20*, 1501.
(15) Meier, D. J. *Polym. Prepr., Am. Chem. Soc., Div. Polym. Chem.* **1977**, *18*, 340.
(16) Gallot, B. R. M. In *Adv. Polym. Sci. Chem.* **1978**, *29*, 85.
(17) Edwards, S. F. *Proc. Phys. Soc. London* **1965**, *85*, 613.
(18) Freed, K. F. *Adv. Chem. Phys.* **1972**, *22*, 1.
(19) Helfand, E. *J. Chem. Phys.* **1975**, *62*, 999.
(20) Hong, K. M.; Noolandi, J. *Macromolecules* **1980**, *13*, 964.
(21) Cahn, J. W.; Hilliard, J. E. *J. Chem. Phys.* **1958**, *28*, 258.
(22) Flory, P. J. "Principles of Polymer Chemistry"; Cornell University Press: Ithaca, N.Y., 1953.
(23) Hashimoto, T.; Todo, A.; Itoi, H.; Kawai, H. *Macromolecules* **1977**, *10*, 377.
(24) Todo, A.; Kiuno, H.; Miyoshi, K.; Hashimoto, T.; Kawai, H. *Polym. Eng. Sci.* **1977**, *17*, 587.
(25) Todo, A.; Hashimoto, T.; Kawai, H. *J. Appl. Crystallogr.* **1978**, *11*, 558.
(26) Stein, R. S., private communication.
(27) Gilmer, J.; Goldstein, N.; Stein, R. S. *Bull. Am. Phys. Soc.* **1980**, *25*, 353.
(28) Debye, P. *J. Chem. Phys.* **1959**, *31*, 680.
(29) Fox, L. "Numerical Solution of Ordinary and Partial Differential Equations"; Addison-Wesley: Reading, Mass., 1962.
(30) Wolfe, P. *Comm. ACM* **1959**, *2*, 12.

Theory of Interfacial Tension in Ternary Homopolymer–Solvent Systems

K. M. Hong* and J. Noolandi*

Xerox Research Centre of Canada, 2480 Dunwin Drive, Mississauga, Ontario, Canada L5L 1J9. *Received October 9, 1980*

ABSTRACT: A recent theory of inhomogeneous multicomponent polymer systems is used to calculate the interfacial tension and width in ternary homopolymer–homopolymer–solvent mixtures. We consider symmetric systems where the polymer–solvent interaction parameters are equal ($\chi_{AS} = \chi_{BS}$), as well as asymmetric systems ($\chi_{AS} \neq \chi_{BS}$). A number of phase diagrams are presented, corresponding to different degrees of miscibility of the components and different values of the molecular weights of the homopolymers. The maxima in the interfacial tension curves as a function of solvent concentration are generally found to be shifted to lower concentrations than the minima in the interfacial width curves. Scaling relations are derived which explain this shift, as well as the dependence of the interfacial tension on molecular weight for symmetric systems. Calculations of the interfacial tension are given for styrene–polystyrene–polybutadiene mixtures.

1. Introduction

The study of polymer compatibility and incompatibility remains an active and important area of applied and fundamental research.[1,2] The development of new techniques of measuring the interfacial tension in multicomponent systems gives a direct quantitative measure of the microscopic compatibility of such systems.[3] In this paper we develop the theory of the interfacial tension in ternary homopolymer–solvent mixtures, which complements the traditional thermodynamic calculations of phase diagram binodal curves.[4,5]

We extend our earlier work on unsymmetrical polymer–polymer interfaces (assuming infinite molecular weight) in the presence of solvent[6] to deal with ternary homopolymer–solvent systems in general. We make use of a new formulation of inhomogeneous multicomponent systems developed recently and discussed in detail elsewhere.[7] Briefly, in our theory we optimize the general free energy functional of the homopolymer–solvent system using the saddle function method, subject to the constraint of no volume change locally upon mixing, and obtain new equations for the mean fields acting on the polymers. These equations are given (without derivation) in section 2 and are expressed in terms of the chemical potential corresponding to a locally homogeneous Flory–Huggins free energy density. The equations are solved numerically by a self-consistent procedure described elsewhere,[7] and phase diagrams are presented for symmetric systems, where the polymer–solvent interaction parameters are equal ($\chi_{AS} = \chi_{BS}$), as well as for asymmetric systems ($\chi_{AS} \neq \chi_{BS}$). Plots of the interfacial tension and width are given for varying amounts of solvent in the system. All of our present calculations are restricted to monodisperse systems.

In order to obtain a better undstanding of the trends observed in the results of the numerical work we develop a number of scaling relations,[8] which are checked against the exact numerical calculations. Although all of our phase diagrams have been studied earlier experimentally[9-12] and theoretically,[4,5,13,14] the corresponding plots of the interfacial tension and width (as well as the interfacial profiles) are presented here for the first time. Finally, we calculate the interfacial tension for a polymerization path in the styrene–polystyrene–polybutadiene system and find good agreement with recent measurements by Reiss and coworkers.[3]

2. Theory

A detailed account of the theory of inhomogeneous multicomponent polymer systems has been presented in an earlier publication.[7] Here we summarize the equations required for the analysis of the ternary homopolymer–homopolymer–solvent mixture. The reader who is interested in the derivation of these equations, as well as a discussion of the theory, is referred to our earlier work.[7]

The mean-field equations for $q_\kappa(x,t)$ (κ = A, B), which is proportional to the probability density that the end of a molecule of type κ and degree of polymerization $Z_\kappa t$ is at x, are

$$\frac{1}{Z_A}\frac{\partial q_A(x,t)}{\partial t} = \frac{1}{6}\frac{\partial^2 q_A(x,t)}{\partial x^2} - \omega_A(x) q_A(x,t)$$
$$\frac{1}{Z_B}\frac{\partial q_B(x,t)}{\partial t} = \frac{1}{6}\frac{\partial^2 q_B(x,t)}{\partial x^2} - \omega_B(x) q_B(x,t) \qquad (2\text{-}1)$$

where x is measured in terms of the Kuhn statistical length b, which is assumed to be the same for the two polymers in model calculations, and Z_κ is the degree of polymeri-

0024-9297/81/2214-0736$01.25/0

zation of the whole molecule.

It is convenient to express all quantities in terms of volume fractions

$$\phi_\kappa = \rho_\kappa/\rho_{0\kappa} \tag{2-2}$$

which are identical with the reduced densities for no volume change upon mixing. The polymer probability densities are related to the volume fraction by

$$\phi_\kappa(x) = \int_0^1 dt\; q_\kappa(x,t)q_\kappa(x,1-t) \tag{2-3}$$

The condition of no volume change upon mixing gives for the solvent volume fraction

$$\phi_S(x) = 1 - \phi_A(x) - \phi_B(x) \tag{2-4}$$

and the boundary conditions for the uniform, bulk phases are[7]

$$q_\kappa(\pm\infty,t) = \exp[t \ln \phi_\kappa(\pm\infty)] \tag{2-5}$$

The initial condition for eq 2-1 is

$$q_\kappa(x,0) = 1 \tag{2-6}$$

The expression for the polymer mean field is obtained from eq 3-13 of ref 7 (including nonlocal terms)

$$\omega_A(x) = \left[F_A(x) - F_A(\pm\infty) - \frac{1}{Z_A} \ln \phi_A(x) \right] - [F_S(x) - F_S(\pm\infty)] + \tfrac{1}{6}[\chi_{AB}\sigma_{AB}^2\phi_B''(x) + \chi_{AS}\sigma_{AS}^2\phi_S''(x) - \chi_{AS}\sigma_{AS}^2\phi_A''(x) - \chi_{BS}\sigma_{BS}^2\phi_B''(x)] \tag{2-7}$$

with a similar expression for $\omega_B(x)$ obtained by interchanging A and B. Of course $\chi_{BA} = \chi_{AB}$, and we assume that the range parameters σ of all the interactions are equal to the average Kuhn length. The functions $F_\kappa(x)$ appear in connection with the expressions for the chemical potential of the "local" homogeneous Flory–Huggins free energy and are defined by

$$F_A(x) = \chi_{AB}\phi_B^2(x) + \chi_{AS}\phi_S^2(x) + (\chi_{AB} + \chi_{AS} - \chi_{BS})\phi_B(x)\phi_S(x) + \frac{1}{Z_A} \ln \phi_A(x) - \left(\frac{\phi_A(x)}{Z_A} + \frac{\phi_B(x)}{Z_B} + \phi_S(x) \right) \tag{2-8}$$

with a similar expression for $F_B(x)$ obtained by interchanging A and B. $F_S(x)$ is defined by

$$F_S(x) = \chi_{AS}\phi_A^2(x) + \chi_{BS}\phi_B^2(x) + (\chi_{AS} + \chi_{BS} - \chi_{AB})\phi_A(x)\phi_B(x) + \ln \phi_S(x) - \left(\frac{\phi_A(x)}{Z_A} + \frac{\phi_B(x)}{Z_B} + \phi_S(x) \right) \tag{2-9}$$

The asymptotic values of the volume fractions $\phi_A(\pm\infty)$, $\phi_B(\pm\infty)$, and $\phi_S(\pm\infty)$ are obtained in the usual way by equating the chemical potential of the various components in the two bulk homogeneous phases; i.e.

$$\begin{aligned} F_A(\infty) &= F_A(-\infty) \\ F_B(\infty) &= F_B(-\infty) \\ F_S(\infty) &= F_S(-\infty) \end{aligned} \tag{2-10}$$

Note that there is a degree of freedom in the description of a ternary system, so that one of the bulk volume fractions, $\phi_A(\infty)$ say, must be specified in order to obtain a unique solution of eq 2-10.

Having specified the boundary conditions through the eq 2-5 and 2-10, we may proceed with the numerical solution of the differential equations (2-1), as described in ref 7, in order to obtain the interfacial density profiles, as well as the interfacial tension, given by eq 3-18 of ref 7

$$\gamma = \int_{-\infty}^{\infty} dx \left[F_S(x) - F_S(\pm\infty) + \frac{1}{6}(\chi_{AB}\sigma_{AB}^2\phi_A'(x)\phi_B'(x) + \chi_{AS}\sigma_{AS}^2\phi_A'(x)\phi_S'(x) + \chi_{BS}\sigma_{BS}^2\phi_B'(x)\phi_S'(x)) \right] \tag{2-11}$$

The results of these calculations, for model as well as real cases, are described in the following section.

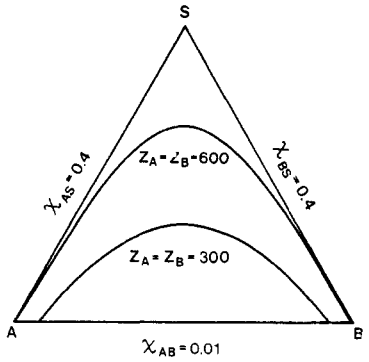

Figure 1. Calculated binodals for a symmetric homopolymer–solvent ternary system with different degrees of polymerization.

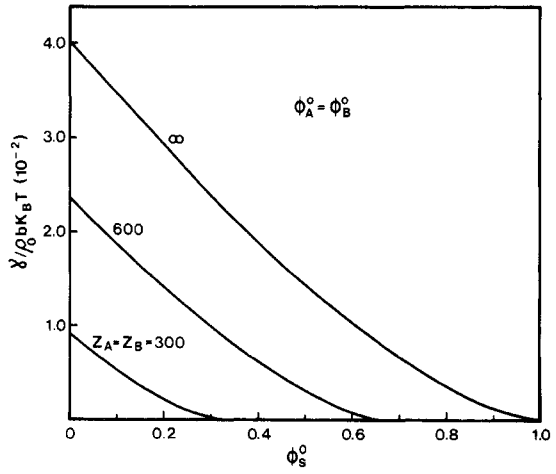

Figure 2. Interfacial tension γ (in reduced units) as a function of total solvent volume fraction for various degrees of polymerization. The curves shown correspond to a trajectory in the phase diagram Figure 1 which is perpendicular to the line AB and passes through the solvent vertex S.

3. Results of Calculations

A. Symmetric Case. Figure 1 shows the calculated binodal curves for $\chi_{AS} = \chi_{BS} = 0.4$, $\chi_{AB} = 0.01$, and different molecular weights. The tie lines in the symmetric case are horizontal and are not shown. With no solvent present, the value of the molecular weight for which 0.01 is the critical value of χ_{AB} is given by[2]

$$\begin{aligned} (\chi_{AB})_{cr} &= \tfrac{1}{2}(1/Z_A^{1/2} + 1/Z_B^{1/2})^2 \\ &= 2/Z \qquad (Z_A = Z_B = Z) \end{aligned} \tag{3-1}$$

so that $Z_{cr} = 200$. For smaller values of Z no phase separation takes place, of course. Figures 2 and 3 show plots of the interfacial tension and width of the interface, corresponding to a trajectory in the phase diagram (Figure 1) which is perpendicular to the line AB and passes through the solvent vertex (i.e., for a mixture with equal volumes of A and B). The width of the interface is defined in the usual way, as the intersection of the tangents to the

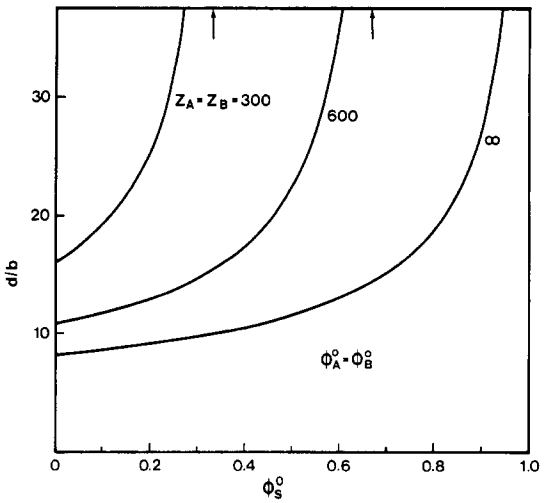

Figure 3. Interfacial width (in units of the Kuhn length b) as a function of total solvent volume fraction for different degrees of polymerization, corresponding to the same trajectory in the phase diagram Figure 1 as indicated for Figure 2.

polymer density profiles at the point midway between the asymptotic bulk values with the values of the polymer densities in the two phases. As expected, the interfacial tensions drop monotonically to zero with increasing solvent concentration. For $Z = \infty$, the interfacial tension vanishes at $\phi_S^0 = 1.0$, since there is no three-phase region in this case for the interaction parameters we have chosen. However, as expected from the phase diagram, for finite molecular weight the interface broadens and the interfacial tension vanishes when the solvent volume fraction reaches the critical value $(\phi_S^0)_{cr}$ given by[2]

$$1 - (\phi_S^0)_{cr} = 2/Z\chi_{AB} \tag{3-2}$$

Although a complete analytical solution for the interfacial density profiles of the homopolymer–homopolymer–solvent system does not exist, it is interesting to compare the above calculations with the known results for the symmetric homopolymer–homopolymer interface with $Z_A = Z_B = \infty$, for which[15]

$$\gamma \propto (\chi_{AB})^{1/2}\rho_0 b k_B T \tag{3-3}$$

and

$$d/b \propto (\chi_{AB})^{-1/2} \tag{3-4}$$

where ρ_0 is the (pure) polymer density in the bulk phase. It can easily be shown that the effect of a small amount of solvent in the symmetric system may be accounted for by the replacement

$$\chi_{AB} \rightarrow \phi_p^0 \chi_{AB} \tag{3-5}$$

where ϕ_p^0 is the total polymer volume fraction, resulting in a "dilution" of the A–B interactions,[15] and this approximation is good when the solvent concentration is approximately constant throughout the system. Using eq 3-5 we then find

$$d/b \propto (\phi_p^0)^{-1/2} \tag{3-6}$$

and replacing ρ_0 by $\phi_p^0\rho_0$ in eq 3-3 we obtain

$$\gamma \propto (\phi_p^0)^{1.5} \tag{3-7}$$

and

$$\gamma d \propto \phi_p^0 \tag{3-8}$$

Equation 3-7 may also be obtained from a scaling argument starting with the general expression for the interfacial tension.

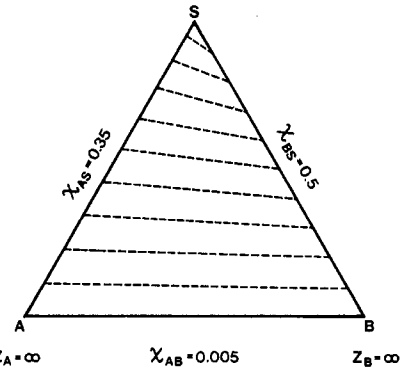

Figure 4. Phase diagram for an asymmetric homopolymer–homopolymer–solvent system with infinite degree of polymerization. The tie lines are drawn for intervals of 0.1 of the total solvent volume fraction in the homopolymer B–solvent phase.

Plots of d/b and γ show that the scaling relations 3-6 and 3-7 are indeed well satisfied for $Z_A = Z_B = \infty$. For $\chi_{AB} = 0.005$ and $\chi_{AS} = \chi_{BS} = 0.4$, the exponents in eq 3-6 and 3-7 are found to be –0.51 and 1.50, while for $\chi_{AB} = 0.1$ we get –0.62 and 1.56. The larger discrepancy between the dilution approximation and the second case is due to the larger repulsion between the two polymers, resulting in a higher concentration of solvent at the interface.

For the symmetric case with finite molecular weight the relation (see Appendix)

$$\gamma d \propto \phi_p^0 - (\phi_p^0)_{cr} \tag{3-9}$$

is satisfied, where the total volume fraction of polymer is

$$\phi_p^0 = \phi_A(\infty) + \phi_B(\infty) \tag{3-10}$$

and the critical value in the symmetric case is[2]

$$(\phi_p^0)_{cr} = 2/Z\chi_{AB} \tag{3-11}$$

Equation 3-8 is a special case of the above for $Z = \infty$. For finite molecular weight we have not been able to obtain an independent relation for the dependence of d on ϕ_p^0. However, the combined relation eq 3-9 shows that a change in the interfacial tension is related to both a change in the volume fraction of polymer and a change in d. This behavior is also observed for the more complicated asymmetric systems ($\chi_{AS} \neq \chi_{BS}$), as discussed later.

B. Asymmetric Case. The phase diagram for $\chi_{AS} \neq \chi_{BS}$ and $\chi_{AB} = 0.005$, with $Z_A = Z_B = \infty$, is shown in Figure 4. Again, no three-phase region occurs since $\chi_{AS} < 0.5$, $\chi_{BS} = 0.5$. The tie lines are drawn for increments of 0.1 of the solvent volume fraction in the homopolymer B–solvent phase. For finite molecular weight, the two-phase region is enclosed by the binodal curve shown in Figure 5. From eq 3-2, $(\chi_{AB})_{cr} = 0.004$ for $Z_A = Z_B = 500$, so that $\chi_{AB} > (\chi_{AB})_{cr}$ in Figure 5. It is interesting to compare Figures 1 and 5. With $\chi_{AB} = 0.005$ and $\chi_{AS} = \chi_{BS} = 0.4$, the binodal for $Z_A = Z_B = 500$ would occupy a small part of the phase diagram shown in Figure 1. However, when $\chi_{AS} = \chi_{BS}$, as shown in Figure 5, the region of incompatibility occupies almost the whole triangle. For very small solvent concentrations the composition of the bulk phase is very similar to what is obtained with no solvent present. The fact that phase separation also takes place for large solvent concentrations results in the "bowing out" of the binodal curve, as shown in Figure 5.

Figure 6 gives plots of the interfacial tension and width corresponding to vertical trajectories through the solvent vertex (i.e., equal volumes of A and B) of the phase diagrams shown in Figures 4 and 5. The interfacial tension

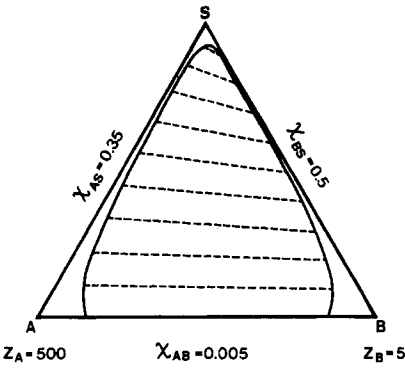

Figure 5. Calculated binodal for the same asymmetric homopolymer–homopolymer–solvent system shown in Figure 4, but with degree of polymerization $Z_A = Z_B = 500$. The right-hand end of the tie lines marks intervals of 0.1 in the total solvent volume fraction.

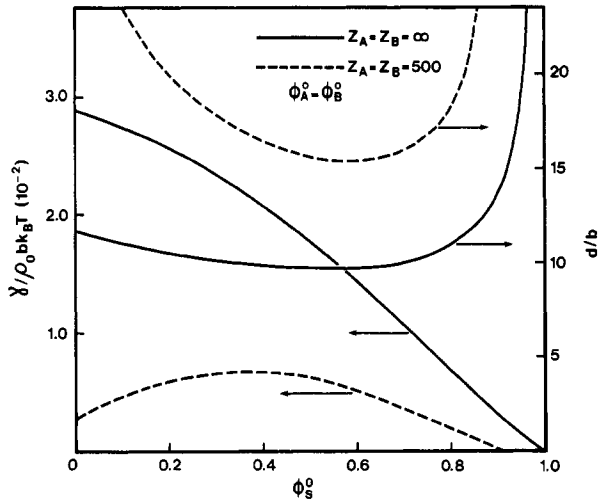

Figure 6. Interfacial tension γ (in reduced units) and interfacial width d (in units of the Kuhn length b) as a function of total solvent volume fraction for different degrees of polymerization, corresponding to trajectories in the phase diagrams Figures 4 and 5 which pass through S perpendicular to AB.

for $Z_A = Z_B = \infty$ drops monotonically to zero, while the corresponding width of the interface remains almost constant until high solvent concentrations are reached. For $Z_A = Z_B = 500$, the interfacial width starts at a finite value for $\phi_S{}^0 = 0$, exhibits a minimum, and diverges for $\phi_p{}^0 \sim 0.9$. The corresponding interfacial tension shows a maximum, which is shifted to the left of the minimum in the interfacial width. The occurrence of the maximum in the interfacial tension curve may be easily understood by referring to Figure 7, where the value of the molecular weight has been chosen so that the lower critical point of the binodal curve touches the line AB. It is clear that in this case the interfacial tension must vanish for $\phi_S{}^0 = 0$. Since γ must also vanish at the upper limit of compatibility, it is not surprising that it shows a maximum at some intermediate value of $\phi_S{}^0$, which marks the region of maximum incompatibility. Figure 5 indicates that for $Z_A = Z_B = 500$ the polymers are incompatible for $\phi_S{}^0 = 0$, and the interfacial tension in this case starts at a value intermediate between $Z_A = Z_B = \infty$ and $Z_A = Z_B = 400$ (Figure 7).

In the Appendix we derive a general formula involving the interfacial tension γ and width d

$$\gamma d \propto \sum_p \left[\phi_p(\infty) + \phi_p(-\infty) - 2\frac{\phi_p(\infty) - \phi_p(-\infty)}{\ln \phi_p(\infty) - \ln \phi_p(-\infty)} \right] \quad (3\text{-}12)$$

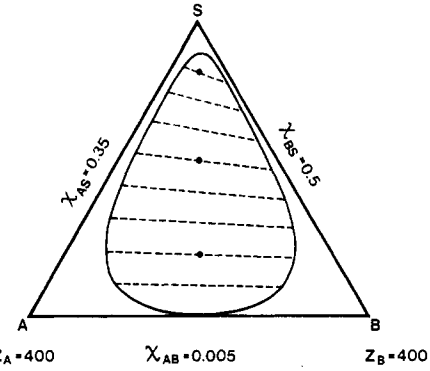

Figure 7. Calculated binodal for the asymmetric homopolymer–homopolymer–solvent system shown in Figures 4 and 5, but with degree of polymerization $Z_A = Z_B = 400$. The dots indicate the total solvent volume fractions for which he interfacial density profiles are shown in Figures 10 and 11.

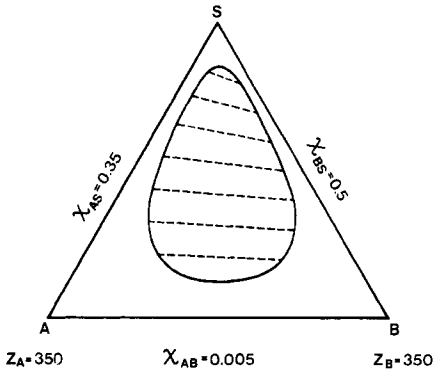

Figure 8. Calculated binodal for asymmetric homopolymer–homopolymer–solvent system shown in previous figures, with degree of polymerization reduced to $Z_A = Z_B = 350$.

The expression in the brackets is a decreasing function with increasing solvent concentration in the region under consideration and shifts the maximum of the interfacial tension curve to the left of the minimum in the interfacial width. For infinite molecular weight the decrease in the interfacial tension shown in Figure 6 is almost entirely due to the decrease in the volume fraction of polymer. The general expression (3-12) reduces to eq 3-9 for the symmetric case, as shown in the Appendix. For the asymmetric case, it can be verified by using the results of our numerical calculations that relation 3-12 is very well satisfied.

As mentioned earlier, Figure 7 shows the phase diagram for $\chi_{AB} = (\chi_{AB})_{cr}$. The evolution of this "egg" diagram as the polymer–solvent parameters are allowed to vary is remarkable. When $\chi_{AS} \to \chi_{BS}$, the egg shrinks to the critical point. However, the shrinkage does not take place uniformly as χ_{AS} approaches χ_{BS}. Referring to an analysis of segregation in regular ternary solutions of small molecules,[13,14] we find the condition for the appearance of the egg from the critical point

$$\left| \chi_{AS} - \chi_{BS} + \frac{Z_A - Z_B}{2Z_AZ_B} \right| > \frac{1}{Z_A{}^{1/2}} + \frac{1}{Z_b{}^{1/2}} \quad (3\text{-}13)$$

where we have introduced a slight generalization into the small-molecule formula to account for the molecular weight of the polymers. According to eq 3-13 the egg does not begin to appear immediately when $\chi_{AS} \neq \chi_{BS}$ but only when this inequality is satisfied. A general analysis of the conditions necessary for the occurrence of the different types of phase diagrams in homopolymer–homopolymer–solvent systems is quite complicated, however, and is be-

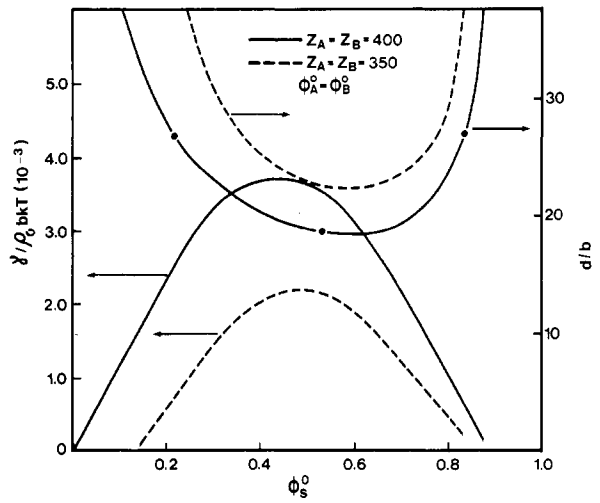

Figure 9. Interfacial tension γ (in reduced units) and interfacial width d (in units of the Kuhn length b) as a function of total solvent volume fraction for different degrees of polymerization, corresponding to trajectories in the phase diagrams Figures 7 and 8 which pass through S perpendicular to AB.

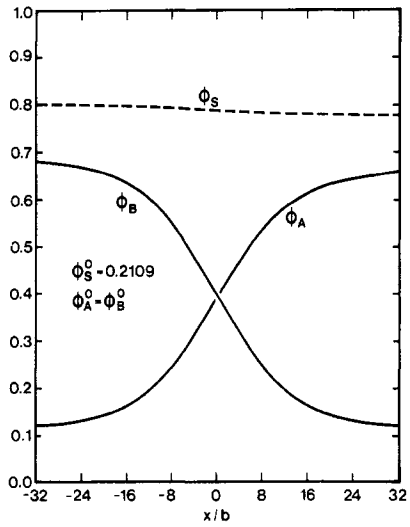

Figure 10. Interfacial volume fractions of polymers (A, B) and solvent (S) corresponding to lowest dot on phase diagram in Figure 7. Note that the solvent volume fraction is measured from the top down. The values of the χ parameters are indicated on the phase diagram, and the distance from the middle of the interface is measured in units of the Kuhn length b.

yond the scope of this paper.

Figure 8 shows the egg diagram when $\chi_{AB} < (\chi_{AB})_{cr}$. For small solvent concentrations the polymers are compatible, and phase separation takes place for larger solvent concentrations only because of the difference in the polymer–solvent interaction parameters. The interfacial tension and width curves for Figures 7 and 8 are given in Figure 9. There is a marked correlation between the minimum in the interfacial width and the maximum in the interfacial tension, as expected from eq 3-12 and the maximum is always shifted to lower values of the solvent volume fraction, as discussed earlier. Note that the surface tension curves in Figure 9 do not always go continuously to zero, because the trajectory on the phase diagram (through S and perpendicular to AB) may not pass exactly through the critical points.

Figures 10 and 11 show the interfacial density profiles corresponding to the three points on the interfacial width curve for $Z_A = Z_B = 400$ (Figure 9). The values of $\phi_S{}^0$ were chosen for convenience to fall on the tie lines drawn in

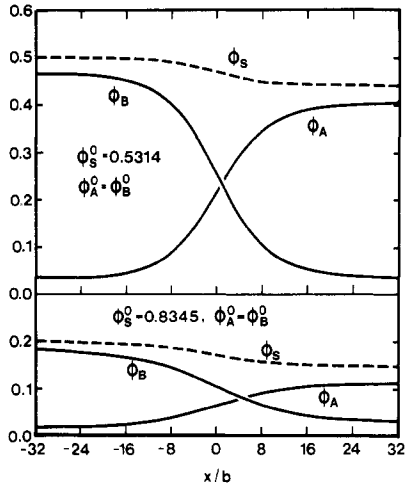

Figure 11. Interfacial volume fractions of polymers (A, B) and solvent (S) corresponding to the higher two dots on phase diagram in Figure 7. The scales in Figures 10 and 11 are chosen to be identical for ease of comparison. Note that the solvent volume fraction is measured from the top down in both panels.

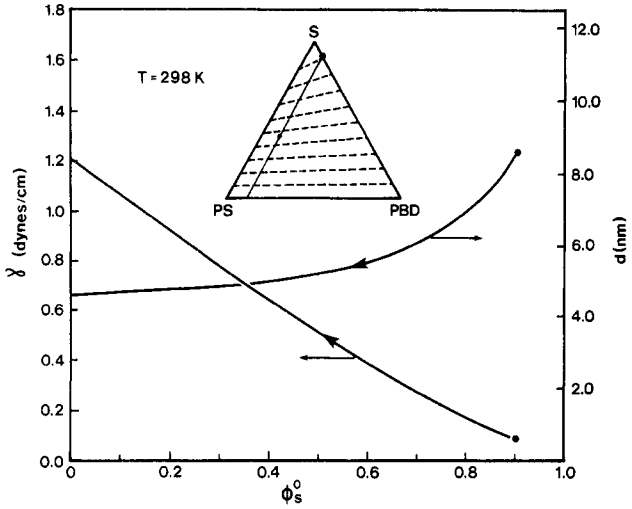

Figure 12. Interfacial tension γ and interfacial width d as a function of total solvent concentration for the path of polymerization shown in the styrene–polystyrene–polybutadiene phase diagram. According to ref 16 $\chi_{PS-S} = 0.49$, $\chi_{PBD-S} = 0.29$, and $\chi_{PS-PBD} = 0.024$ (using the reference volume for styrene) at $T = 298$ K.

Figure 7. As the solvent concentration increases, the density profiles show a narrowing of the interface until for large concentrations the effect of the solvent causes a diffuse broadening. For intermediate solvent concentrations the interfacial profiles appear as if there were an increased effective χ interaction parameter between the homopolymers. It would be interesting to study this effect from an analytical treatment of the problem.

C. Styrene–Polystyrene–Polybutadiene. As a final example we calculate the interfacial tension and width for the polymerization path of high-impact polystyrene[16] as shown on the styrene–polystyrene–polybutadiene phase diagram (Figure 12). In this calculation we have assumed that the volume fraction of styrene which has polymerized at some point in the phase diagram has formed chains of high molecular weight polystyrene which are in thermodynamic equilibrium. While this is a crude approximation to the actual polymerization kinetics, it should still give us some idea of the variation of the interfacial width and tension along the polymerization path. In addition, the degree of polymerization of the PBD was taken to be in-

finite, since M_w = 149 000 and M_w/M_n = 1.46.[16]

Starting with $\phi_{PBD}^0 = 0.1$, $\phi_{PS}^0 = 0$, and $\phi_S^0 = 0.9$ for the path shown in the phase diagram, the reaction terminates with $\phi_{PBD} = 0.116$, $\phi_{PS}^0 = 0.884$, and $\phi_S^0 = 0$. The polymerization path is a straight line, as may be easily verified from the equations describing the path

$$\begin{aligned} \phi_{PBD}^0(f) &= \phi_{PBD}^0(0)/D(f) \\ \phi_{PS}^0(f) &= f(\rho_S/\rho_{PS})[1 - \phi_{PBD}^0(0)]/D(f) \\ \phi_S^0(f) &= (1 - f)[1 - \phi_{PBD}^0(0)]/D(f) \\ D(f) &= \phi_{PBD}^0(0) + [1 - f + f(\rho_S/\rho_{PS})][1 - \phi_{PBD}^0(0)] \end{aligned} \tag{3-14}$$

where f is the fraction of styrene converted to polystyrene. Since polystyrene is more compact than styrene ($\rho_S < \rho_{PS}$), the total volume of the system decreases and hence ϕ_{PBD}^0 increases with f even though the amount of polybutadiene is constant.

For the styrene monomer, we used ρ_S = 0.008 72 mol cm^{-3},[17] while for polystyrene, ρ_{PS} = 0.0103 mol cm^{-3} [18] and b_{PS} = 7.1 Å.[17] For polybutadiene we have ρ_{PBD} = 0.0176 mol cm^{-3} [17] as an average density and b_{PBD} = 6.8 Å.[17] The χ parameters (for T = 298 K) are taken from the paper by Kruse,[16] $\chi_{PS\text{-}S}$ = 0.49, $\chi_{PBD\text{-}S}$ = 0.29, and $\chi_{PS\text{-}PBD}$ = 0.024, using the reference volume of styrene as well as the quoted solubility parameters. We have assumed that the χ values are independent of concentration, grafting, and cross-linking, all of which may be important in high-impact polystyrene, as noted by Kruse.[16] For this system the interfacial tension increases by more than an order of magnitude as the polymerization proceeds, and it would be interesting to attempt to correlate this change with the rheological properties of the material. From Figure 12 we note also that the decrease in the interfacial width by a factor of 2 agrees approximately with the increase in the interfacial tension predicted by eq 3-8, although in this case $\chi_{PS\text{-}S} \neq \chi_{PBD\text{-}S}$. For $\phi_S^0 = 0.9$, we predict $\gamma \simeq 0.1$ dyn/cm, in good agreement with recent measurements by Riess.[3]

4. Discussion

Phase diagrams of the type shown in Figure 5 (or Figure 1) occur when the polymers are incompatible in the bulk but each is miscible in a solvent. An example of such a system is polystyrene–polypropylene–toluene.[10] When the components are pairwise miscible in all proportions but phase separation takes place at some composition when all three are mixed, we obtain a phase diagram like Figures 7 and 8. Examples most often quoted are benzene–butyl rubber–EPDM rubber and diphenyl ether–atactic polypropylene–linear polyethylene.[11] In our calculations we also studied phase diagrams for which the polymers are incompatible in bulk and only one of the polymers is miscible with the solvent in all proportions.[2] However, our attempts to obtain a closed miscibility envelope as well as a miscibility gap for the bulk polymers were unsuccessful. The reason for this is probably our use of χ parameters, which were assumed to be completely independent of concentration. With the relaxation of this constraint it should be possible to calculate binodals for the more complicated miscibility gaps.

To summarize our calculations of the binodals, the results agree with earlier work[4,5] in that at high polymer concentrations the polymer–polymer interaction (χ_{AB}) controls the amount of miscibility, while at low polymer concentrations the difference between the polymer–solvent interaction parameters (χ_{AS} and χ_{BS}) is responsible for the phase separation. Finally, for a small interaction between the polymers, a closed miscibility gap occurs if the polymer–solvent interaction parameters are different, as in Figure 7. We also see that decreasing the molecular weight of the polymers for fixed χ_{AB} has the same effect as lowering χ_{AB} at fixed molecular weight, since $(\chi_{AB})_{cr}$ is related to Z_A and Z_B through eq 3-1.

We have presented calculations of the interfacial tension and interfacial width for the different phase diagrams discussed above. In general, we found that the nonlocal terms had a negligible effect on the results and could be safely ignored. Scaling relations were derived for the dependence of the interfacial tension on the polymer volume fractions and the width of the interface. Although approximate, the simple scaling laws are useful in understanding the results of the more complicated calculations.

Data on direct measurements of the interfacial tension in ternary systems are difficult to find. Langhammer and Nestler[9] have carried out experiments on poly(vinyl acetate)–chlorinated poly(vinyl chloride)–ethyl oxalate as a function of concentration and molecular weight, but not all the χ parameters are known for this system, making comparison with our theory impossible at this time. An earlier approximate analysis of the Langhammer and Nestler data has been made by Vrij.[19] We have also calculated the interfacial tension for a path of polymerization in the polystyrene–polybutadiene–styrene system, using a rough model for the polymerization kinetics and neglecting the effects of grafting and cross-linking. Good agreement with recent measurements of the interfacial tension in this system by Riess[3] is obtained for large molecular weights and high styrene volume fraction.

Acknowledgment. We thank L. M. Marks for developing the computer programs used to evaluate the interfacial density profiles and related quantities and for assistance with the numerical calculations.

Appendix

Here we derive the approximate scaling law eq 3-12. We begin with the result for the interfacial tension γ, given in ref 7

$$\gamma = \sum_p \frac{\rho_{0p} b_p^2}{3} \int dx \int_0^1 dt \, \frac{\partial q_p}{\partial x} \frac{\partial q_p^\dagger}{\partial x} \tag{A-1}$$

where the nonlocal terms (whose contributions are usually small) have been neglected and

$$q_p^\dagger(x,t) = q_p(x,1 - t) \tag{A-2}$$

Using the values of the probability densities in the bulk phases, eq 2-5, we approximate the gradient at the interface by

$$\frac{\partial q_p}{\partial x} \simeq \frac{\exp[t \ln \phi_p(\infty)] - \exp[t \ln \phi_p(-\infty)]}{d} \tag{A-3}$$

and carry out the integrations in eq A-1, giving

$$\gamma d \propto \sum_p \left[\phi_p(\infty) + \phi_p(-\infty) - 2\frac{\phi_p(\infty) - \phi_p(-\infty)}{\ln \phi_p(\infty) - \ln \phi_p(-\infty)} \right] \tag{A-4}$$

For the symmetric case with infinite molecular weight, this result reduces to

$$\gamma d \propto \phi_p^0 \tag{A-5}$$

where ϕ_p^0 is the total volume fraction of polymer, as found earlier from eq 3-6 and 3-7. For finite molecular weight, with $\chi_{AS} = \chi_{BS}$ and $Z_A = Z_B = Z$, we get from eq A-4

$$\gamma d \propto \phi_p^0 - (\phi_p^0)_{cr} \tag{A-6}$$

where now

$$\phi_p^0 = \phi_A(\infty) + \phi_B(\infty) \quad \text{(A-7)}$$

and the critical value of the polymer volume fraction is given by[2]

$$(\phi_p^0)_{cr} = 2/Z\chi_{AB} \quad \text{(A-8)}$$

The above result (eq A-6) can be easily derived from eq 2-10 for the symmetric case ($\chi_{AS} = \chi_{BS}$). For the asymmetric case no simplification of eq A-4 takes place.

References and Notes

(1) Olabisi, O.; Robeson, L. M.; Shaw, M. T. "Polymer-Polymer Miscibility"; Academic Press: New York, 1979.
(2) Krause, S. In "Polymer Blends"; Paul, D. R., Newman, S., Eds.; Academic Press: New York, 1978; Vol. 1, p 15.
(3) Riess, G. MMI Symposium on Polymer Compatibility and Incompatibility, Midland, Mich., 1980 (to be published).
(4) Zeman, L.; Patterson, D. *Macromolecules* **1972**, *5*, 513.
(5) Hsu, C. C.; Prausnitz, J. M. *Macromolecules* **1974**, *7*, 320.
(6) Hong, K. M.; Noolandi, J. *Macromolecules* **1980**, *13*, 964.
(7) Hong, K. M.; Noolandi, J., to be published.
(8) de Gennes, P. G. "Scaling Concepts in Polymer Physics"; Cornell University Press: Ithaca, N.Y., 1979.
(9) Langhammer, G.; Nestler, L. *Makromol. Chem.* **1965**, *88*, 179. See also: Silberberg, A.; Kuhn, W. *Nature (London)* **1952**, *170*, 450. *J. Polym. Sci.* **1954**, *13*, 21.
(10) Berek, D.; Lath, D.; Durdovic, V. *J. Polym. Sci., Part C* **1967**, *16*, 659.
(11) Koningsveld, R.; Kleintjens, L. A.; Schoffeleers, H. M. *Pure Appl. Chem.* **1974**, *39*, 1.
(12) Aharoni, S. *Macromolecules* **1978**, *11*, 277.
(13) Meijering, J. L. *Philips Res. Rep.* **1950**, *5*, 333.
(14) Meijering, J. L. *Philips Res. Rep.* **1951**, *6*, 183.
(15) Helfand, E.; Tagami, Y. *J. Chem. Phys.* **1972**, *56*, 3592.
(16) Kruse, R. L. In "Copolymers, Polyblends, and Composites"; Platzer, N. A. J., Ed.; American Chemical Society: Washington, D.C., 1975, p 141.
(17) Brandrup, J., Immergut, E. H., Eds. "Polymer Handbook"; Interscience: New York, 1966.
(18) Höcker, H.; Blake, C. J.; Flory, P. J. *Trans. Faraday Soc.* **1971**, *67*, 2252.
(19) Vrij, A. *J. Polym. Sci., Part A-2* **1968**, *6*, 1919.

Excluded-Volume Effects in Dilute Polymer Solutions. 11. Tests of the Two-Parameter Theory for Radius of Gyration and Intrinsic Viscosity

Y. Miyaki and H. Fujita*

Department of Macromolecular Science, Osaka University, Toyonaka, Japan.
Received December 2, 1980

ABSTRACT: The two-parameter theory for radius of gyration and intrinsic viscosity was tested with experimental data on polystyrene and polyisobutylene published in preceding parts of this series. It was found that the radius expansion factors of the two polymers in different solvents gave a composite curve when plotted against the excluded-volume parameter z, as required by the two-parameter theory. This curve was best fitted by the Domb–Barrett empirical equation. For either polymer, the viscosity expansion factors in different solvents as functions of z did not give a single curve. This implies that intrinsic viscosity does not always obey the two-parameter theory.

One of the most important achievements in modern polymer science is the development of the two-parameter theory for molecular properties of linear flexible polymers in dilute solution. Much work has been done in the past 3 decades to check the predictions of this theory by experiment. The principal results are best summarized and discussed in Yamakawa's monograph.[1] A careful study of them leads us to the conviction that the validity of the two-parameter theory, especially on hydrodynamic properties, is not as yet definitively established.

The purpose of this paper is to check it for mean-square radius of gyration $\langle S^2 \rangle$ and intrinsic viscosity at zero shear rate $[\eta]$, mostly using experimental data on polystyrene and polyisobutylene accumulated in our laboratory during the past few years. Except for ones taken from the doctoral thesis of Y. Miyaki, these data were published in preceding parts of this series of papers.

Criteria for the Two-Parameter Theory

According to this theory, the radius expansion factor α_s for linear flexible polymers at infinite dilution should be a universal function of a single variable z called the excluded-volume parameter; i.e.

$$\alpha_s = \alpha_s(z) \quad (1)$$

where α_s and z are defined by

$$\alpha_s^2 = \langle S^2 \rangle / \langle S^2 \rangle_0 \quad (2)$$

$$z = (4\pi \langle S^2 \rangle_0 / M)^{-3/2} M_0^{-2} M^{1/2} \beta \quad (3)$$

with $\langle S^2 \rangle$ and $\langle S^2 \rangle_0$ the mean-square radii of gyration of a linear flexible polymer in the perturbed and unperturbed state, respectively, M the molecular weight of the polymer, M_0 the molecular weight of its repeat unit, and β the binary cluster integral representing the strength of interaction between a pair of repeat units. The term "universal" in the above statement means that a quantity is independent of the kind of polymer and solvent condition. A solvent condition is defined by the kind of solvent and the temperature.

If, as was assumed by Flory,[2] the polymer molecule in solution behaves as if it were impermeable to solvent, the two-parameter theory predicts that the viscosity expansion factor α_η also should be a universal function of z; i.e.

$$\alpha_\eta = \alpha_\eta(z) \quad (4)$$

where α_η is defined by

$$\alpha_\eta^3 = [\eta]/[\eta]_0 \quad (5)$$

with $[\eta]$ and $[\eta]_0$ the intrinsic viscosities of a polymer in the perturbed and unperturbed state, respectively.

If eq 1 and 4 hold, there should exist a universal relation between α_s and α_η. As can be seen in Yamakawa's book,[1] previous tests with well-documented experiments are

0024-9297/81/2214-0742$01.25/0